water

MDPI

Article

Study of Condensate Absorption Capacity in Exposed Soil when Water Recedes at the Bottom of Hoh Xil Lake, Qinghai

Bei Li [1,2], Liang Zhu [1], Xi Chen [1], Jingtao Liu [1,*], Yuxi Zhang [1] and Wanpeng Shi [1,3]

[1] Institute of Hydrogeology and Environmental Geology, Chinese Academy of Geological Sciences, Shijiazhuang 050061, China; libei@mail.cgs.gov.cn (B.L.); zhuliang@mail.cgs.gov.cn (L.Z.); chenxi@mail.cgs.gov.cn (X.C.); zhangyuxi@mail.cgs.gov.cn (Y.Z.); wanpeng0910@163.com (W.S.)
[2] Key Laboratory of Groundwater Contamination and Remediation, China Geological Survey (CGS) & Hebei Province, Shijiazhuang 050061, China
[3] School of Water Resources and Environment, China University of Geosciences, Beijing 100083, China
* Correspondence: liujingtao@mail.cgs.gov.cn

Abstract: In order to investigate the characteristics of the condensate absorption capacity in an exposed sandy bottom when water recedes, the characteristics of condensate variation, condensate formation time, condensate volume, and its absorption capacity were investigated in July 2021, using a micro-osmometer. The research area was the artificial water-retention layer and bare ground of the exposed sandy bottom, formed under the influence of the warming-wetting trend that occurs when water recedes in the salt-lake area of the Qinghai-Tibet Plateau, as well as two conditions: underpass and under sealed. According to the results, the time of condensation generation during the observation period in the salt-lake area of Hoh Xil begins at about 0:00 and ends at about 10:00 The artificial water-retention layer had little influence on the condensation generation time, and the trend of the condensation rate is the same. The unidirectional condensation of water in near-surface air is significantly better under artificial water-retention layer conditions than under bare ground conditions, with condensation occurring three times more frequently than under bare ground conditions. The amount of water condensation in the lower part of the soil under artificial aquifer conditions is 2.588 times greater than that in the near-ground air, while the amount of water condensation in the lower part of the soil under bare ground conditions is 1.783 times greater than that in the near-ground air. The total amount of bi-directional condensation under artificial water-retention layer conditions is slightly less than that in bare ground conditions, while the total amount of unidirectional condensation under artificial water-retention layer conditions is significantly higher, indicating that the artificial water-retention layer contributes to the absorption of water from near-surface air. Due to the presence of permafrost in the Qinghai-Tibet Plateau region, the zero-flux surface transport of evanescent heat in the salt-lake area of Hoh Xil lies approximately within 30 cm from the surface to the ground. The analogous humidity coefficient characterizes the condensate absorption capacity coefficient as the storage capacity of condensate in the surface layer of the soil in a certain area, providing strong evidence that the condensate absorption capacity is higher under the artificial water-retention layer conditions than in bare ground, regardless of whether the condensation is bi-directional or unidirectional. The results of this study can provide a theoretical basis for condensate absorption capacity and vegetation restoration in the bare ecologically degraded areas of the lake bottom.

Keywords: receding waters in the lake; sandy area; condensation; micro-osmometer; artificial water-retention layer; water absorption capacity

check for updates

Citation: Li, B.; Zhu, L.; Chen, X.; Liu, J.; Zhang, Y.; Shi, W. Study of Condensate Absorption Capacity in Exposed Soil when Water Recedes at the Bottom of Hoh Xil Lake, Qinghai. *Water* **2022**, *14*, 1433. https://doi.org/10.3390/w14091433

Academic Editor: Maria Mimikou

Received: 31 March 2022
Accepted: 28 April 2022
Published: 29 April 2022

1. Introduction

In September 2011, the natural outburst of Zhuonai Lake in the Hoh Xil hinterland of the Qinghai-Tibet Plateau, after the water level had risen continuously for years [1,2] became a typical example of lake changes in the Qinghai-Tibet Plateau region in the context of global warming and wetting. The outburst of Zhuonai Lake led to the interconnecting of four lakes downstream, including Kusai Lake, Haidingnuoer Lake, and Salt Lake. The interconnecting of these lakes resulted in a sudden reduction of more than 100 km^2 in the size of Zhuonai Lake [3–5], as well as a yearly expansion of the lake surface area after the water level of Salt Lake rose sharply [6]. In 2019, according to the analysis of the meteorological conditions of past years, Salt Lake may be at risk of overflowing under extreme rainfall conditions [7]. In order to avoid the natural overflow of Salt Lake, which could affect the six lifelines, including the Qinghai-Tibet Highway and Qinghai-Tibet Railway, as well as a number of transmission lines and optical cables, the China Geological Survey conducted several expert discussions on the rising water level of Salt Lake. Several special reports were submitted to the Ministry of Natural Resources following the discussions, which attracted the attention of government leaders. In August 2019, after making multi-period predictions on the equilibrium of Salt Lake water level, a diversion project was carried out. After the water was released from the lake, the water level of Salt Lake was effectively controlled and the risk of outburst has been mitigated.

The outbrust of Zhuonai Lake has led to the exposure of a large area at the lake bottom, as well as the formation of a new sandy area. Coupled with the abnormal climate and frequent windy weather in Hoh Xil, this has led to the continuous development of natural disasters such as wind and sand storms in the Zhuonai Lake area [8]. Years of continuous erosion by the mobile cover of wind and sand will cause hazards such as grass degradation. Since the outburst of Zhuonai Lake and the implementation of the diversion project, the surface area of Salt Lake has undergone the process of rapid expansion to slow expansion to a slow contraction. This process will gradually form a new exposed area of the lake bottom. In order to avoid the formation of a large sandy area in the Salt Lake area similar to that of Zhuonai Lake, it is of great import to take effective measures to stop further sanding in the early stages of desertification.

Dew refers to the liquid water formed by condensation of vapor water in the atmosphere as well as pore water in the ground and surface soil when the surface temperature and surface temperature reach the dew point, which is a component of soil water. The natural conditions such as the intense temperature difference between day and night and the relative humidity of the air are the important factors affecting its production. In arid and extremely arid conditions, any replenishment of water resources can have a positive impact on ecosystems in arid regions where water resources are scarce. Dew, as a stable and continuous water resource, plays a very important role in maintaining the stability of the ecosystem in arid and semi-arid areas, although the amount of water is small [9,10]. Dew is an important water source for soil crusts of some plants, insects, small animals, and organisms in an arid environment, which can improve the germination rate of plant seeds and effectively reduce the water loss caused by soil evaporation. Many scholars at home and abroad have done a lot of research on dew. The formation mechanism and influencing factors of dew are discussed [11–13], but how to make efficient use of dew is rarely reported.

As one of the many water-saving materials, a water-retaining agent can absorb more than 100 times or more water than its own weight, and has continuous water absorption capacity, which can be applied to the soil for a long time, and with no pollution. The water-retaining agent in the soil fixes the water by absorbing water and expanding it. When the soil is short of water, the effective water absorbed by the soil can be released by osmotic pressure, in time to maintain the soil water condition and for crops to absorb and use. After applying the water-retaining agent to the soil, it absorbs water and expands, aggregates the discrete soil particles into a group, increases the soil porosity, reduces the soil bulk density, and regulates the three-phase balance of the soil. Since the water-retaining agent molecules contain active groups that can adsorb and exchange ions, the ions adsorbed by the water-retaining agent can fix the fertilizer nutrients and achieve the effect of a slow and controlled release of fertilizer. With its advantages of low cost, good gel strength, and environmental friendliness [14–16] a mineral-composite water-retaining agent gradually began to be applied in flower breeding, fruit tree transplanting and water conservation in agriculture and forestry.

Based on this, this paper selects the exposed sandy area of the Hoh Xil Lake where the water recedes in Qinghai to observe condensation generation patterns and absorption effects, thereby enriching the research content related to condensation hydrology in sandy areas of different genesis in China while also aiming to provide basic data for the rational management, utilization, and ecological restoration of fragile ecosystems.

2. Overview of the Research Area and Research Background

The Hoh Xil Salt Lake area is deeply inland, with high terrain, thin air, and high mountains to the north and south. It is located in a semi-enclosed terrain, causing oceanic winds to have little influence. The climate is characterized as dry, cold, and windy with low rainfall, showing significant continental climate characteristics. The average annual temperature of Hoh Xil is −10.0 °C~4.1 °C, and the minimum temperature is −46.2 °C. The distribution trend is decreasing gradually from southeast to northwest. The coldest month is January, and the warmest month is July. The average annual precipitation is 173–495 mm, decreasing gradually from southeast to northwest. Precipitation is mainly concentrated in May to September, accounting for more than 90% of the annual precipitation. The average annual wind speed distribution increases gradually from the southeast and northeast to the hinterland and the west, and the contour line is basically in the shape of a "trumpet mouth". The wind speed is between 8.0 and 3.5 m/s. Modern glaciers are widespread in Hoh Xil, with 255 glaciers covering 750.7 square kilometers and ice reserves of 81.6489 billion cubic meters. The reserve is located in the permafrost zone, which accounts for more than 90% of the area of the reserve and is up to 400 m thick. Glaciers and frozen soil are huge reservoirs of solid soil. Salt Lake, also known as 68 Daoban Salt Lake [17], is located in the north-eastern part of the Hoh Xil National Nature Reserve on the Qinghai-Tibet Plateau. This location is approximately 220 km from Golmud in the north and 8 km from the Qinghai-Tibet Railway (highway) in the east and is under the administrative division of Zhiduo County, Yushu Tibetan Autonomous Prefecture, Qinghai Province. It is also part of the Yangtze River Source Park of Sanjiangyuan National Park. A large part of the Salt Lake basin makes up the core conservation area of Sanjiangyuan National Park, while Kusai Lake, Haidingnuoer Lake, and the northern shore of the Salt Lake, to both sides of the Qinghai-Tibet Railway, are the traditional use zone.

Haidingnuoer, Kusai, and Zhuonai Lakes are located in order from east to west on the northwest side of Salt Lake. Prior to the outburst of Zhuonai lake in September 2011, all the other three lakes were closed lakes [18]. Among them, the main tributary of Zhuonai Lake was Zhuonai River, which originated from the meltwater of the Five Snow Peaks glacier. the main tributary of Kusai Lake was Kusai River from the Kunlun Mountains' Great Snow Peaks and Xueyue Mountain, while Haidingnuoer Lake is mainly recharged by seasonal rivers and surface runoffs. Following the outburst of Zhuonai Lake, the Kusai-Haidingnuoer chain of outflows rapidly expanded the surface area of Salt Lake and created rivers between them. According to the results of the survey in March 2020, the areas of the lake bottom that were exposed after the Zhuonai Lake outburst were mainly located in the shallow water areas in the west and south of the original lake, in addition to a relatively small patch of exposed area in the northern region, where the topography slopes to a large receding body of water. The exposed areas of the lake bottom were mostly the areas that were inundated by the rapid rise of the lake water before the outburst and the areas inundated by the stable water of the lake for a long time before the outburst., covering an area of about 87 km^2 and accounting for 75.6% of the entire exposed lake bottom area. The Salt Lake area, with the rapid expansion of the Zhuonai Lake outburst and the gradual reduction in artificial diversions, will form a new exposed lake bottom area in the receding water area. The soil and water conservation of the top soil is particularly important in the early stages of desertification, one of the most important procedures of preventing desertification [19]. The strong evaporation, as well as the low and scattered rainfall in the Hoh Xil region, severely hinders soil and water conservation as well as the revegetation of the surface soil in the receding lake bottom. At the same time, the strong light and large diurnal temperature differences in the Hoh Xil region provide favorable conditions for condensation formation [20–25]. To investigate the effect of rainfall and condensate absorption capacity in the Hoh Xil region, the author added a mineral composite water-retention agent, developed by the Laboratory of Pollution Mechanisms and Remediation of the China Geological Survey, to the surface soil of the receding area and used the artificial water-retention layer it formed as the main research subject to conduct a study on rainfall and condensate absorption capacity in the receding area of the lake bottom [16]. This will provide a research direction for the efficient use of soil condensate in the local desert area of Hoh Xil.

3. Materials and Methods

3.1. The Experimental Materials

Mineral-composite water-retaining agent is a kind of polymer composite, containing a large number of -OH, -COOH, and other strong hydrophilic groups. Acrylic acid is in situ polymerized between bentonite mineral layers, to obtain a milky-white-translucent water-absorbing resin. The addition of minerals improves the defect of the water-absorbing material synthesized by small molecular organic matter, greatly enhances the gel strength of the product, and reduces the production cost. The product was developed by the author in the Pollution Mechanism and Remediation Laboratory of China Geological Survey. The product has been approved as a Chinese invention patent and has been widely used in many site-remediation projects. Mineral-compound water-retaining agent has a strong association with water, and its water absorption rate can reach 150–700 times. It can absorb water repeatedly, release water, absorb fertilizer, keep fertilizer, and release slowly, increasing the fertilizer effect, drug effect, loose soil, and other effects, so has been widely used in agriculture and forestry drought resistance and water conservation, soilless cultivation, desertification prevention and control, urban greening, and other fields [14,15]. Therefore, it is of great significance for the authors to add mineral-composite water-retention agent as a soil–water-retention agent to the soil surface, to study the soil–water retention in an exposed desert area.

3.2. Experimental Methods

The experiment was conducted using the weighing method [9,23], with 24 h uninterrupted observations for a period of six days, from 4 July to 9 July 2021. The experimental apparatus utilized a 7.5-cm diameter PVC pipe as the inner tube and a 10 cm PVC pipe as the outer tube. The test tubes were divided into two types: under sealed and underpass [26]. The underpass tubes were sealed with a 400-mesh fleece screen, to ensure the permeability of the water vapor under the ground, as well as maintain the quality of the soil inside the test tubes. Meanwhile, the under sealed tubes were sealed with a plastic film, to insulate the air pocket under the ground from water vapor interference. See Figure 1 for the experimental setup.

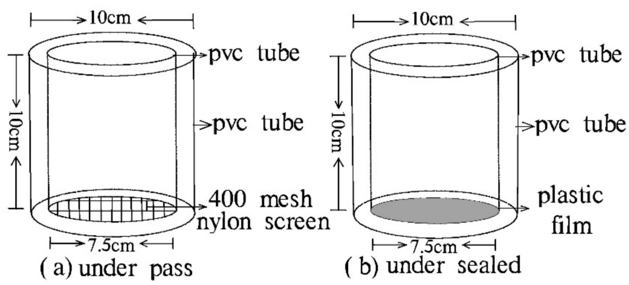

Figure 1. Experimental setup (**a**) is the under pass tube. PVC pipe with a diameter of 7.5 cm is used as the inner cylinder and PVC pipe with a diameter of 10 cm is used as the outer cylinder. The bottom

of the inner cylinder is sealed with 400 mesh wool screen, while the outer cylinder is not sealed. (**b**) is the under sealed tube. PVC pipe with a diameter of 7.5 cm is used as the inner tube and PVC pipe with a diameter of 10 cm is used as the outer tube. The bottom of the inner tube is sealed with plastic film, while the outer tube is not sealed.

The experiments were set up into two groups: the control group (CK), i.e., the bare ground (original soil filling); and the artificial water-retention-layer group, i.e., the application and mixing of the mineral-composite water-retention agent to the 0–5 cm surface layer of soil (the application ratio is 30 kg/mu). As seen in Table 1 of the experimental setup, the experimental group was further divided into the artificial water-retention layer, made by mixing mineral-composite water-retention agent and original soil placed 0–5 cm from the surface. Care should be taken when making the test tubes, to ensure that the inner tube is flush with the ground surface and the outer tube is slightly higher than the ground surface, to avoid allowing any surface soil to enter the tubes. The inner tube was taken out at each hour, weighed and measured with an electronic balance with an accuracy of 0.01 g, after which the data were recorded. The temperature and humidity data were also recorded at their corresponding times.

Table 1. Experimental arrangement table.

	Underpass		**Under Sealed**	
	0–5 cm	CK	0–5 cm	CK
Experimental group	C1	M	C4	N
Parallel group	F1	P	F4	Q

Note: C1 and F1 indicate that the artificial water-retaining layer is formed by mixing the mineral-compound water-retaining agent 30kg/mu with the matrix soil, and filling the mixed soil into the 0–5 cm position in the upper part of the lower general test cylinder; M and P represent the bottom type test cylinder is directly filled with matrix soil, without adding mineral-compound water-retaining agent; C4 and F4 represent, according to the application ratio of mineral-composite water-retaining agent 30 kg/mu, mixed with the matrix soil to form an artificial water-retaining layer, and the mixed soil is filled into the 0–5 cm position in the upper part of the lower sealing test cylinder. N and Q indicate that the bottom sealing test cylinder is directly filled with matrix soil without adding mineral-compound water-retaining agent.

3.3. Calculating the Volume of Condensate

During the observation period, the mass of the underpass and under sealed test tubes increased and decreased with every corresponding time interval. This is because the bottom of the under sealed test tubes were sealed with film, and their mass changed as the result of the exchange of water vapor in the air and soil in the test tubes. The mass increase indicates the water vapor in the air entering the soil, suggesting the occurrence of condensation. A decrease in the mass of the test tubes indicates that water vapor from the tubes was entering the air, suggesting the occurrence of evaporation. The bottom of the underpass test tubes was sealed with mesh fleece screen, which does not influence the water vapor exchange between the test tubes and the bottom of the tubes. When the mass of the test tubes increases, it means that there is water vapor in the air and under the ground condensing to the surface. When the mass of the test tubes decreases, it indicates that evaporation is the dominate force. The amount of condensation expressed in mass was then converted to condensation expressed in height [9,13], which was calculated as:

$$H = 10m/\rho\pi r^2$$

where, H is the condensation volume (mm); m is the change in sample mass (g); r is the internal diameter of the micro-osmometer (cm); and ρ is the density of water (g/cm^{-3}).

During the experiment, weather station data were used to monitor indicators such as ground temperature, air temperature, relative humidity, and wind speed in real time.

4. The Influence of the Condensate Generation Pattern

The research area is located at an altitude of 4500 m above sea level in an alpine anoxic zone, and there are often fierce animals such as coyotes in the uninhabited area.

Thus, due to these hostile working conditions in the research area, this field observation on condensation was carried out in July, when the ultraviolet light is strong and evaporation is strong. Preliminary meteorological data collection, data calculation, test tube preparation, equipment burial, and other preparatory work took about 15 days. The experiment was carried out over a period of five days from 16:00 on 4 July to 14:00 on 9 July, taking into account the necessity of continuous operation at high altitude.

4.1. Influence of Sources of Condensation Generation

There are two main sources of water vapor that can develop into condensation airborne water vapor or water vapor originating from a soil pore space above a certain depth below the surface [27–30]. Both methods of condensation exist in the Hoh Xil area, as evidenced by the daily condensate generation observed in the underpass and under sealed test tubes. At 8:00 on 5 July, the condensation of the underpass and under sealed test tubes in the artificial water-retention layer was 0.078 mm and 0.030 mm, respectively. The condensation of underpass and under sealed test tubes in the bare ground was 0.072 mm and 0.041 mm, respectively. The amount of soil pore water vapor condensation was significantly greater than the amount of air condensation, with water vapor condensation of soil under the artificial water-retention layer being 2.588 times greater than the amount of air condensation near the ground. Meanwhile, water vapor condensation of the soil under the bare ground was 1.783 times greater than the amount of air condensation near the ground. Thus, the content of the condensation is dominated by water vapor in the soil pores, but the air condensation is also a non-negligible source of moisture (Figure 2).

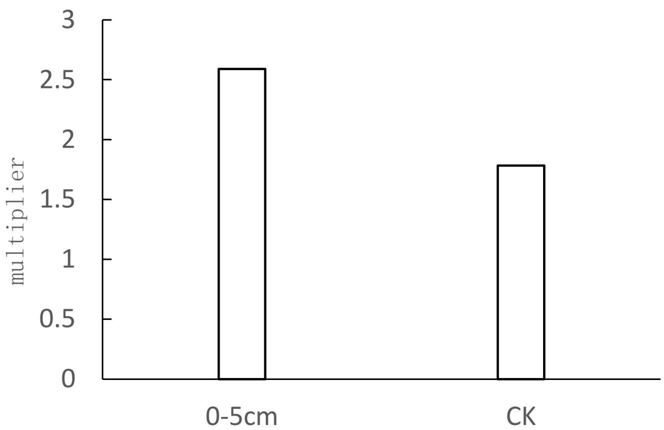

Figure 2. Comparison graph of condensate generation multipliers.

4.2. The Influence of Condensation Generation Time

During the observation period of 16:00 on 4 July to 14:00 on 6 July, condensation was observed under rainfall-free conditions, with continuous condensation mainly occurring from 0:00 to 8:00 on 6 July. The water vapor condensation trends in both directions were basically the same for the nearground air and underground, with slightly different patterns of unidirectional condensation in the near-ground air. When comparing the underpass test tubes of the artificial water-retention layer and bare ground, condensation for both places began at 0:00 and continued until 8:00. Meanwhile, condensation in the bare ground tubes continued until 10:00, with the rate of condensation increasing and then decreasing. However, condensation occurred at 0:00, 4:00, and 8:00 in the artificial water-retention layer tubes, only at 2:00. in the bare ground tubes. The frequency of condensation was three times higher in the artificial water-retention layer than in the bare ground (Figure 3). Based on the monitoring data of the near-surface air temperature and ground temperature at different depths, the surface soil temperature was higher than the near-surface air temperature for most of the daytime in the Hoh Xil area due to strong UV light, which was not conducive to the generation of condensation. As the sun gradually set in the evening, the surface soil temperature began to drop. When the surface soil temperature was lower than the near-ground temperature, water vapor was transported towards the surface by the temperature gradient; in other words, condensation began to occur. Within the soil, the cooling rate of the surface soil was faster than that of the deep soil. Due to this, the water vapor in the pores of the deeply buried soil was transported towards the surface, so the amount of condensation in the underpass test tubes was greater than that in the under sealed test tubes. Moreover, the artificial water-retention layer with the addition of the mineral-composite water-retention agent had some insulation properties in addition to water-retention properties [31–33]. After early-morning solar irradiation, the warming was slightly faster and condensation ended earlier compared to the control group.

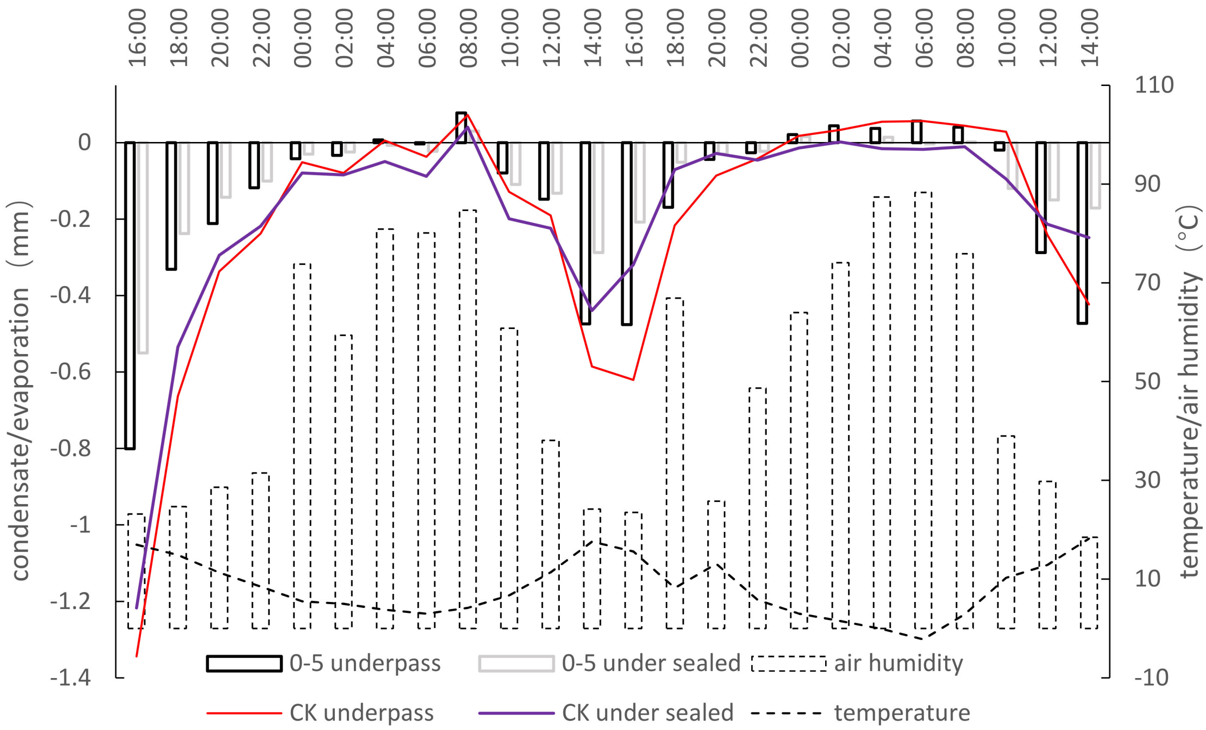

Figure 3. Condensate generation time.

4.3. The Influence of the Condensate Generation Volume

The variation of the condensate generation in the presence of the artificial water-retention layer and bare ground during the observation period was also studied. According to the experimental results recorded from 16:00 on 4 July to 14:00 on 6 July, the total amount of condensate generated by the micro-osmometer was 0.284 mm in the underpass test tubes of the artificial water-retention layer and 0.312 mm in the bare ground, while the total amount of condensate generated by the under sealed tubes was 0.062 mm and 0.042 mm, respectively. The total condensate generation volume for underpass test tubes in the artificial water-retention layer was less than that of the bare ground test tubes. The results of this study are consistent with Professor Guo Bin's findings that condensate generation is greatest in bare ground compared to other sub-bedding conditions, and that different sub-bedding surfaces result in different amounts of condensate generation. Accordingly, the total condensate generation volume for the under sealed test tubes in the artificial water-retention layer was larger than that in the test tubes in the bare ground, indicating that the artificial water-retention layer has a beneficial effect on the absorption of water vapor from the near-ground air (Figure 4).

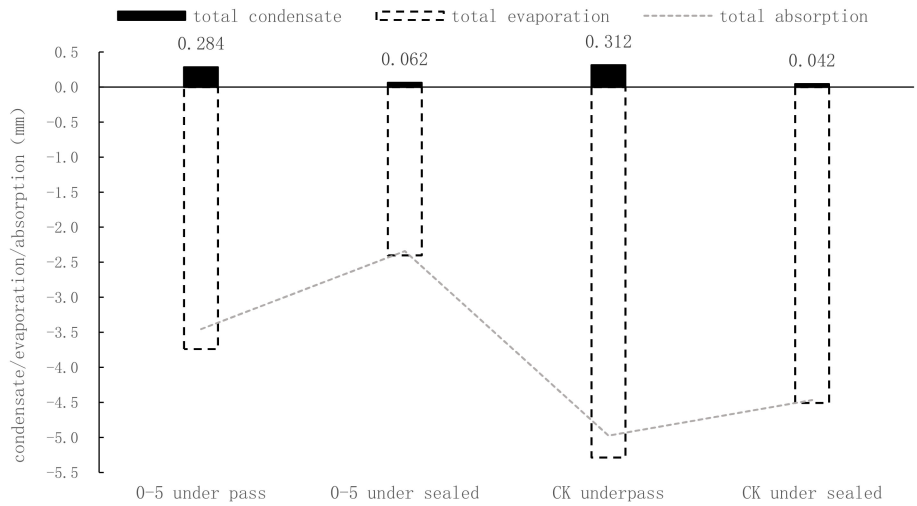

Figure 4. Condensate generation volume.

5. Ground Temperature Transport Patterns

The author set up meteorological stations to monitor air temperature, humidity, rainfall, and snow melt in the experimental research area and buried soil temperature and humidity sensors 5 cm, 10 cm, 20 cm, 30 cm, and 50 cm away from the ground surface. Synchronous air and ground temperature monitoring data showed that the surface cooling rate was higher than the deep soil cooling rate, and when the surface temperature was lower than the deep soil temperature, a dissipative zero-flux surface was formed below the surface. In other words, the temperature at a certain depth below the ground presents the highest value in the vertical profile. The soil temperature above and below this zero-flux surface was lower than the ground temperature at that depth, which was the dissipative zero-flux surface [13,34,35]. Driven by the temperature gradient, water vapor in the soil pore space above the heat zero-flux surface was transported towards the surface and became a source of water vapor for surface–soil condensation [36]. The location of the zero-flux surface changed with time, during diurnal alternation [37].

According to the analysis of the monitoring data collected during the period from 16:00 on 5 July to 14:00 on 6 July, there was a transportation pattern of the position of the zero-flux surface of heat in the range of 5 cm to 50 cm underground. After a long period of ultraviolet radiation at the surface from 16:00 until 20:00, the temperature of soil 5 cm underground was the highest, and the temperature of soil 50 cm underground was the lowest. Water vapor in the soil pores mainly evaporates into the atmosphere, and then is transported to an even deeper location (Figure 5). As the sun sets around 21:00–22:00 in the salt-lake area of Hoh Xil, the surface temperature gradually decreases with the sunset. Based on an analysis of the monitoring data, the soil temperature of 13 °C at 10 m under the ground was the highest value recorded at 22:00 on 5 July. This value was higher than the soil temperature of the upper and bottom parts of the lake and is conducive to the formation of condensate. As the day progressed to 2:00 on 6 July, the dispersion zero-flux surface moved down to 30 cm below ground level, after which the maximum ground temperature was recorded at this location until 10:00. The difference between the surface soil temperature and the zero-flux surface temperature gradually increased before the sun rose (the sun rises in the Hoh Xil Salt Lake area roughly between 06:00 to 08:00). After the sun rose, the ground was radiated by UV light. The surface soil temperature began to rise at 8:00 and reached 11.1 °C at 5 cm below ground level by 12:00, at which point the zero-flux surface jumped from 30 cm under the ground to the surface, where it remained until sunset. The daily temperature transport process of the subsurface zero-flux surface alternated in this way. The above analysis of the zero-flux surface transport process shows that the transport pattern of water vapor in soil between 22:00 at night and 10:00 in the morning coincided with the time of condensation generation observed in the micro-osmometer test tubes, further confirming that the water vapor in the soil pore space is an important source of condensation generation.

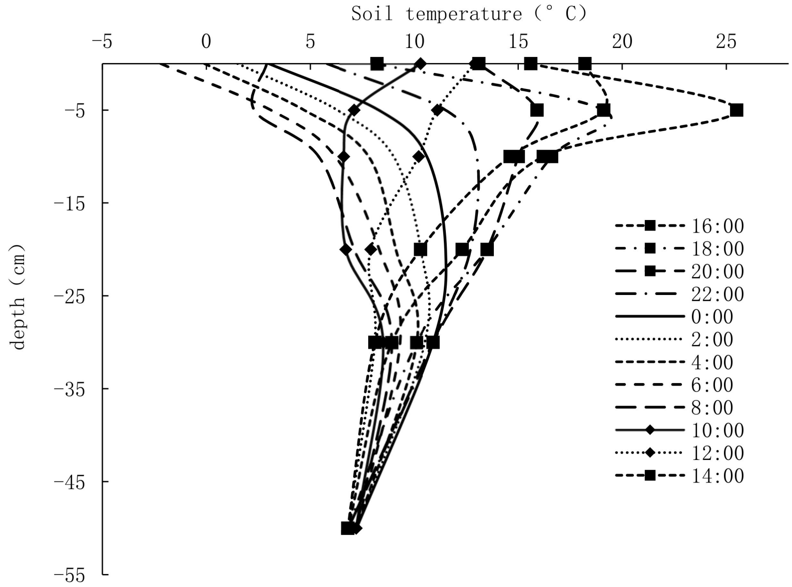

Figure 5. Soil temperature transport patterns near the surface.

6. Condensation Absorption Effect

According to an analysis of the rule of condensation and water vapor transport in soil, evaporation and condensation always alternate. Once condensation ends, evaporation begins immediately. Water that continues to condense through the night will accumulate on the surface of the soil and rapidly dissipate into the air with exposure to ultraviolet radiation after sunrise [20,21]. This part of the water cycle, although small, is extremely important for the restoration of grassland of the sandy areas formed at the beginning when the water of the lake recedes. During the observation period, in the underpass and under sealed test tubes under the condition of artificial water-retention layer and bare ground, the ratio of total evaporation to total condensation of the four types of test tubes were significantly different (Table 2). The multiplier of the unidirectional condensation test tubes of near-ground air, in particular, showed a pattern of magnitude difference. According to the data, the total evaporation of underpass test tube in the artificial water-retention layer was 13.17 times the amount of total condensation, while the total evaporation of the bare ground was 16.93 times the amount of total condensation. This result shows that the artificial water-retention layer plays an important role in maintaining the effect of the two-way condensation state. The total evaporation of the artificial water-retention layer under sealed test tube was 38.91 times the total condensation, while the total evaporation of the bare ground was 106.50 times that of the total condensation. Thus, under the condition of unidirectional condensation of water vapor in the near-ground air, the artificial water-retention layer is extremely effective in absorbing and holding the condensed water in the surface soil.

Table 2. Ratio of total evaporation to total condensation for each type of test tubes.

	Artificial Water-Retention Layer—Underpass	Artificial Water-Retention Layer—Under Sealed	Bare Ground—Underpass	Bare Ground—Under Sealed
Multiplier	13.17	38.91	16.93	106.50

The coefficient of wetness is the reciprocal of drought index and is usually expressed as the ratio of the amount of surface water precipitation to evaporation, i.e., $K = P/E$ (where coefficient of wetness is K, precipitation is P, evaporation is E). Similar to the coefficient of wetness, the author used the ratio of total amount of condensate to total amount of evaporation continuously observed over a number of days in the micro-osmometer test tubes, to characterize the absorption capacity of condensate under different conditions in the area as follows:

$$K_D = D/E$$

where, coefficient of condensate absorption is K_D, amount of condensate is D, and amount of evaporation is E.

According to the analysis of the experimental observation data, the coefficient of condensate absorption of the underpass test tubes in the artificial water-retention layer and the bare ground was 0.0759 and 0.0591, respectively (Figure 6). Meanwhile, the absorption capacity of the artificial water-retention layer in the bi-directional condensation was 1.29 times that of the bare ground. The coefficient of condensate absorption of the under sealed test tubes in the artificial water-retention layer and the bare ground was 0.0257 and 0.0094, respectively. The absorption capacity of the artificial water-retention layer in the unidirectional condensation was 2.74 times that of the bare ground (Figure 7). For vegetation in arid areas, especially in the bare ground of the lake bottom at the beginning of sandification, the condensate absorption capacity is of great ecological significance to the water supply and growth of shallow-rooted plants.

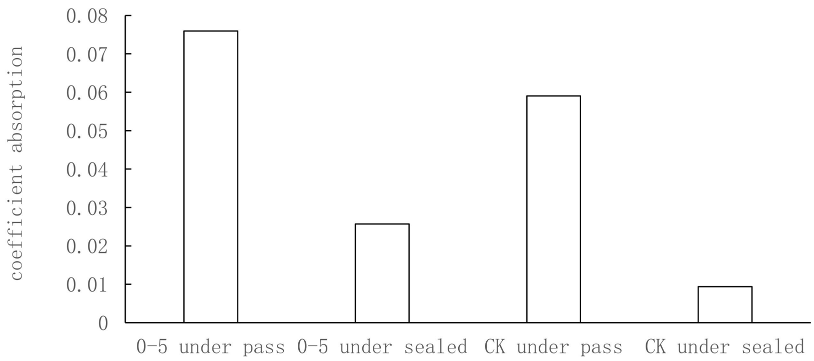

Figure 6. Comparison of coefficient of condensation.

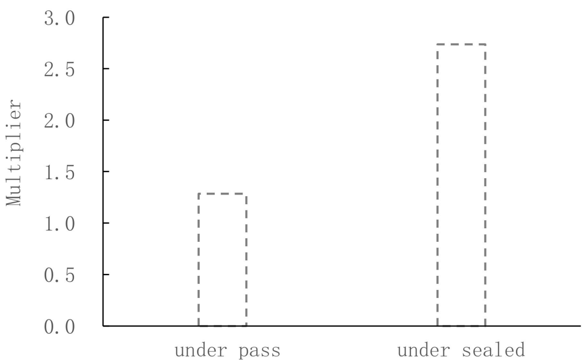

Figure 7. Comparison of the absorption capacity of the artificial water-retention layer.

7. Conclusions

(1) Condensate exists in the Hoh Xil Salt Lake area, and there are two sources of soil condensation: condensation from atmospheric water vapor and condensation from deep soil pores. The amount of water vapor condensation in the lower part of the soil in the artificial water-retention layer conditions was 2.588 times the amount of condensation in the air near the ground, while the amount of water vapor condensation in the lower part of the bare ground was 1.783 times the amount of condensation in the air near the ground.

(2) The artificial water-retention layer in the salt-lake area of Hoh Xil had little influence on the time of condensation generation, as it ended only slightly earlier than the bare

ground, and the trend of the condensation rate remained the same. However, the unidirectional condensation of water vapor in the near-surface air in the artificial water-retention layer was significantly better than that of the bare ground, and the frequency of condensation was three times higher than that of the bare ground.

(3) The total amount of bi-directional condensation in the artificial water-retention layer was slightly less than that of the bare ground, while the total amount of unidirectional condensation in the artificial water-retention layer was significantly higher than that of the bare ground. Together, this data indicates that the artificial water-retention layer helped to promote the absorption capacity of water vapor in the near-surface air.

(4) Due to the existence of permafrost in the Qinghai-Tibet Plateau region, the zero-flux surface transport of heat dissipation in the salt-lake area of Hoh Xil lies approximately within 30 cm to the surface.

(5) The analogous coefficient of wetness, which characterizes the coefficient of condensate absorption as the storage capacity of condensate in the surface layer of soil in a certain area. It strongly demonstrated that the condensate absorption capacity of the artificial water-retention layer in the Hoh Xil Salt Lake area was higher than that of bare ground, regardless of whether it was bi-directional or unidirectional condensation, with the absorption multipliers being 1.29 and 2.74 times, respectively.

Author Contributions: Data curation, L.Z.; investigation, X.C. and W.S.; methodology, J.L.; project administration, Y.Z.; writing—original draft, B.L. All authors have read and agreed to the published version of the manuscript.

Funding: This study was supported and funded by the Basic Scientific Research Operations Fund of the Chinese Academy of Geological Sciences (No. SK202116), the Hydrogeological Investigation of the China Geological Survey (No. D2021504003), and the Hebei Province Outstanding Youth Science Fund (No. DD20190331).

Institutional Review Board Statement: Not applicable.

Informed Consent Statement: Not applicable.

Data Availability Statement: The data was available on the request from the corresponding author.

Acknowledgments: We would like to thank the anonymous reviewers for their valuable comments and guidance on the manuscript. We are grateful to researcher Liu Jingtao for his guidance throughout the process and to the Suonan Dajie Protection Station of Sanjiangyuan National Park administration bureau for their help.

Conflicts of Interest: The authors declare no conflict of interest.

References

1. Zhang, Y.; Xie, C.; Zhao, L.; Wu, T.; Pang, Q.; Liu, G.; Wang, W.; Liu, W. The formation of permafrost in the bottom of the Zonag Lake in Hoh Xil on Qinghai-Tibet Plateau after an outburst: Monitoring and simulation. *J. Glaciol. Geocryol.* **2017**, *39*, 949r–956r.
2. Li, S.J. The scientific expedition on the modern lake evolution in the Qinghai-Tibet Plateau: A preliminary report. *J. Lake Sci.* **1998**, *10*, 95–96.
3. Liu, B.; Lin, L.I.; Yue, D.U.; Liang, T.; Duan, S.; Hou, F.; Ren, J. Causes of the outburst of Zonag Lake in Hoh Xil, Tibetan Plateau, and its impact on surrounding environment. *J. Glaciol. Geocryol.* **2016**, *38*, 305–311.
4. Wang, Y.B.; Liu, X.Q.; Yang, X.D.; Zhang, E.L.; Matsumoto, R. A 4000-year moisture evolution recorded by sediments of Lake Kusai in the Hoh Xil area, northern Tibetan Plateau. *J. Lake Sci.* **2008**, *20*, 605–612.
5. Yao, X.; Liu, S.; Sun, M.; Guo, W.; Zhang, X. Changes of Kusai Lake in Hoh Xil region and causes of its water overflowing. *Acta Geogr. Sin.* **2012**, *67*, 689–698.
6. Yao, X.; Sun, M.; Gong, P.; Liu, B.; Li, X.; An, L.; Ma, C. Overflow probability of the salt lake in Hoh Xil region. *J. Geogr. Sci.* **2018**, *28*, 647–655. [CrossRef]
7. Liu, W.H.; Xie, C.W.; Wang, W. Analysis on expansion trend and outburst risk of the Yanhu Lake in Hoh Xil region, Qinghai-Tibet Plateau. *J. Glaciol. Geocryol.* **2019**, *41*, 1–12.
8. Xie, C.W.; Liu, W.H.; Wu, J.C.; Yang, G.; Zhang, Y.; Wang, W.; Liu, G. Environmental changes caused by the outburst of Zonag Lake and the possible outburst model of Yanhu Lake in the Hoh Xil region. *J. Glaciol. Geocryol.* **2019**, *41*, 1–16.
9. Guo, B.; Chen, Y.N.; Hao, X.M.; Li, B.F.; Cao, Z.C. Characteristics of soil condensation water and its influencing factors on different underlying surfaces in the lower reaches of the Tarim River. *J. Nat. Resour.* **2011**, *26*, 1963–1974.

10. Zhao, L.; Li, S.; Zhao, Z.; Yu, X.; Sun, L.; Zhao, P. Temporal and spatial evolution and regional difference analysis of urban ecological efficiency in arid and semiarid areas. *Arid. Land Geogr.* **2020**, *43*, 449–457.
11. Guo, H.; Qian, Y.; Yuan, G.X.; Wang, C.X. Research progress on the soil vapor extraction. *J. Groundw. Sci. Eng.* **2020**, *8*, 57–66.
12. Chen, R. Source of Soil Condensation Water in the Gurbantunggut Desert. *J. Desert Res.* **2012**, *32*, 985–989.
13. Sun, Z.; Yu, S.; Zhou, A.; Zhang, J.; Yang, L. Experimental Study on the Condensation Water in Lop Nur Region, Xinjiang. *Geol. Sci. Technol. Inf.* **2008**, *27*, 91–95.
14. Sun, X.X.; Zheng, D.J. Evaluation of Water Retention and Repeated Water Absorption Performance of 10 Different Super Absorbent Polymers (SAPs). *For. Technol.* **2022**, *47*, 35–39.
15. Liu, Y.; Geng, D.D.; Han, Y.S. Environment-friendly Superabsorbent: Development, Property and Application. *Chin. Agric. Sci. Bull.* **2022**, *38*, 86–90.
16. Li, B. Study on preparation of acrylic acid-bentonite water retaining agent and its water retaining effect. *Jiangsu Agric. Sci.* **2018**, *46*, 289–292.
17. Dongsheng, H. Investigation and study on lake resources in Kekexili region. *Arid. Land Geogr.* **1992**, *15*, 50–58.
18. Luo, C.G.; Han, F.Q.; Pang, X.P.; Zhou, J. Study on sublacustrine morphology of main lakes in Hoh Xil region. *J. Salt Lake Res.* **2010**, *18*, 1–8.
19. Amiraslani, F.; Dragovich, D. Combating desertification in Iran over the last 50 years: An overview of changing approaches. *J. Environ. Manag.* **2011**, *92*, 1–13. [CrossRef]
20. Zhang, J.; Zhang, Y.; Downing, A.; Cheng, J.; Zhou, X.; Zhang, B. The influence of biological soil crusts on dew deposition in Gurbantunggut Desert, Northwestern China. *J. Hydrol.* **2009**, *379*, 220–228. [CrossRef]
21. Pan, Y.; Wang, X.; Zhang, Y. Dew formation characteristics in a revegetation-stabilized desert ecosystem in Shapotou area, Northern China. *J. Hydrol.* **2010**, *387*, 265–272. [CrossRef]
22. Temina, M.; Kidron, G.J. Lichens as biomarkers for dew amount and duration in the Negev Desert. *Flora-Morphol. Distrib. Funct. Ecol. Plants* **2011**, *206*, 646–652. [CrossRef]
23. Groh, J.; Slawitsch, V.; Herndl, M.; Graf, A.; Vereecken, H.; Pütz, T. Determining dew and hoar frost formation for a low mountain range and alpine grassland site by weighable lysimeter. *J. Hydrol.* **2018**, *563*, 372–381. [CrossRef]
24. Kool, D.; Agra, E.; Drabkin, A.; Duncan, A.; Fendinat, P.; Leduc, S.; Lupovitch, G.; Nambwandja, A.; Ndilenga, N.; Thị, T.N.; et al. The overlooked non-rainfall water input sibling of fog and dew: Daily water vapor adsorption on a! Nara hummock in the Namib Sand Sea. *J. Hydrol.* **2021**, *598*, 126420. [CrossRef]
25. Tomaszkiewicz, M.; Abou Najm, M.; Zurayk, R.; El-Fadel, M. Dew as an adaptation measure to meet water demand in agriculture and reforestation. *Agric. For. Meteorol.* **2017**, *232*, 411–421. [CrossRef]
26. Yin, R.; Wu, Y.; Zhang, X.; Ha, S.; Tian, X.; Li, Z.; Wang, J.; Miao, H.; Ren, J. Effects of biological crusts on dew deposition and evaporation in the southern edge of the mu us sandy land, northern china. *Acta Ecol. Sin.* **2013**, *33*, 6173–6180.
27. Jinlong, Z.; Aboduola, A.; Xianguang, D. An experimental study on the condensation water in the plain area of the northern slope of T ianshan Mountains. *J. Xinjiang Agric. Univ.* **2002**, *25*, 49–53.
28. Jia, R.; Li, X.; Liu, L.; Pan, Y.; Gao, Y.; Wei, Y. Effects of sand burial on dew deposition on moss soil crust in a revegetated area of the Tennger Desert, Northern China. *J. Hydrol.* **2014**, *519*, 2341–2349. [CrossRef]
29. Guo, Z.; Jing, E.; Nie, Z.; Jiao, P.; Dong, H. Analysis on the characteristics of soil moisture transfer during freezing and thawing period. *Adv. Water Sci.* **2002**, *13*, 298–302.
30. Kidron, G.J.; Starinsky, A. Chemical composition of dew and rain in an extreme desert (Negev): Cobbles serve as sink for nutrients. *J. Hydrol.* **2012**, *420*, 284–291. [CrossRef]
31. Woodhouse, J.; Johnson, M.S. Effect of superabsorbent polymers on survival and growth of crop seedlings. *Agric. Water Manag.* **1991**, *20*, 63–70. [CrossRef]
32. Behera, S.; Mahanwar, P.A. Superabsorbent polymers in agriculture and other applications: A review. *Polym.-Plast. Technol. Mater.* **2020**, *59*, 341–356. [CrossRef]
33. Nnadi, F.; Brave, C. Environmentally friendly superabsorbent polymers for water conservation in agricultural lands. *J. Soil Sci. Environ. Manag.* **2011**, *2*, 206–211.
34. Luchen, L.; Ziyang, G.; Shugao, Q.; Yuqing, Z.; Liang, L.; Kaijie, Y. Foliar condensate absorption capacity of four typical plant species and their physiological responses to water in the Mu Us Sandy Land of northwestern China. *J. Beijing For. Univ.* **2021**, *43*, 72–80.
35. Wei, C.; Yu, S.; Jichun, W.U.; Jing, L.I.; Shengting, W. Spatial variability of permafrost soil-moisture on the slope of the Qinghai-Tibet Plateau. *Adv. Water Sci.* **2017**, *28*, 32–40.
36. Wang, W.H.; Wu, T.H.; Li, R.; Xie, C.W.; Zhu, X.F. An overview of advances on moisture migration of the active layer in permafrost regions of the Qinghai-Tibetan Plateau. *J. Northwest Norm. Univ.* **2017**, *53*, 102–111.
37. Hu, G.; Zhao, L.; Li, R.; Wu, T.; Pang, Q.; Wu, X.; Qiao, Y.; Shi, J. Characteristics of hydro-thermal transfer during freezing and thawing period in permafrost regions. *Soils* **2014**, *46*, 355–360.